Shear-Induced Nano-Macro Structural Transition in a Polymeric Bicontinuous Microemulsion

Kasiraman Krishnan,[1] Kristoffer Almdal,[3] Wesley R. Burghardt,[4] Timothy P. Lodge,[1,2] and Frank S. Bates[1]
[1]*Department of Chemical Engineering and Materials Science, University of Minnesota, Minneapolis, Minnesota 55455*
[2]*Department of Chemistry, University of Minnesota, Minneapolis, Minnesota 55455*
[3]*Risø National Laboratory, DK-4000 Roskilde, Denmark*
[4]*Department of Chemical Engineering, Northwestern University, Evanston, Illinois 60208*

(Received 6 February 2001; published 9 August 2001)

Bicontinuous microemulsions arise in a narrow concentration range for ternary blends containing two immiscible homopolymers and the corresponding diblock copolymer. Steady shear reveals four distinct regimes of response as a function of shear rate, corresponding to flow-induced transitions in fluid structure. *In situ* neutron scattering shows flow-induced anisotropy in the nanometer-scale microemulsion structure at moderate shear rates, while higher rates induce bulk phase separation, with micron-size morphology, which is characterized with *in situ* light scattering and optical microscopy.

DOI: 10.1103/PhysRevLett.87.098301 PACS numbers: 82.70.Kj, 61.12.Ex, 64.75.+g

Soft materials often exhibit complex equilibrium morphologies arising from a subtle balance of intermolecular forces. Stresses induced by shear flow are capable of disrupting these balances, leading to flow-induced deformation of equilibrium morphologies, or even flow-induced transitions to nonequilibrium phases. There are numerous examples of shear-induced structural transitions in virtually all classes of complex fluids, including surfactants [1,2], liquid crystals [3], block copolymers [4,5], colloids [6], and polymer solutions and blends [7,8].

Bicontinuous microemulsions (BμE) are a particularly intriguing class of material in which amphiphilic molecules stabilize the interface between immiscible liquids with compositional heterogeneity on the nanometer scale. We recently demonstrated that BμE may be generated in polymers by preparing nearly symmetric blends of two immiscible polymers with a corresponding diblock copolymer [9]. Microemulsion phases are found in the region of the phase diagram where mean-field theory anticipates an isotropic Lifshitz point, and are stabilized by concentration fluctuations that are ignored in mean-field theory [9,10]. Since shear can strongly impact polymer phase behavior through its coupling to concentration fluctuations [4,7], we expect that polymeric BμE will exhibit rich behavior under flow. These fluids resemble the sponge phases consisting of a 3D bilayer of surfactant separating domains of solvent, in which a shear-induced sponge-lamellar phase transition is reported [1]. They also resemble fluctuating disordered symmetric diblock copolymers, where shear can induce a transition to an ordered lamellar phase [4]. However, they also are similar to polymer blends, where shear can strongly influence the multiphase morphology and promote either shear-induced mixing or demixing [8]. Based on these precedents, it is not immediately clear which response(s) the BμE will exhibit. In this Letter we demonstrate that shear first distorts the BμE structure and then induces a bulk phase separation by which the length scale of concentration heterogeneity increases by 2 orders of magnitude. Further increases in shear rate apparently drive the system towards remixing.

The BμE described here contains poly(ethyl ethylene) (PEE), poly(dimethyl siloxane) (PDMS), and a PEE-PDMS diblock copolymer with molecular weights (g/mol) of 1710, 2130, and 10 400 ($f_{\mathrm{PEE}} = 0.52$), respectively, and low polydispersities ($M_w/M_n \leq 1.1$). The PEE was obtained by saturating precursor 1,2-polybutadiene with deuterium, in both the homopolymer and diblock copolymer samples, thereby enhancing the system neutron contrast. A detailed description of the synthesis procedures and the phase diagram is available elsewhere [11]. The pure PEE-PDMS material exhibits an order-disorder transition at 90 °C, while the PEE-PDMS binary mixture has a critical temperature of 150 °C. The experiments discussed in this Letter were conducted on a BμE containing 10% block copolymer and equal amounts of homopolymers by volume.

Steady shear rheological measurements, performed using a Rheometrics Scientific ARES controlled-strain rheometer, reveal four regimes in its mechanical response to flow (Fig. 1); identical viscometric properties are obtained upon increasing or decreasing the shear rate. At low shear rates (Regime I), the microemulsion exhibits Newtonian behavior, but as the shear rate is increased, shear thinning becomes evident (Regime II). Further increase in shear rate leads to a regime in which the shear stress is nearly constant (Regime III), while at the highest rates studied, the stress once again increases with shear rate (Regime IV). We will provide a detailed analysis of this complex rheology in a future publication. Here we simply note that all three components are disentangled, and the viscoelastic response (including normal forces) is dominated by the interfacial structure.

To characterize the structural changes responsible for this unusual rheology, we have used *in situ* small-angle neutron scattering (SANS), small-angle light scattering (SALS), and optical microscopy. The SANS experiments were conducted with the 30 m NSF/CHRNS SANS

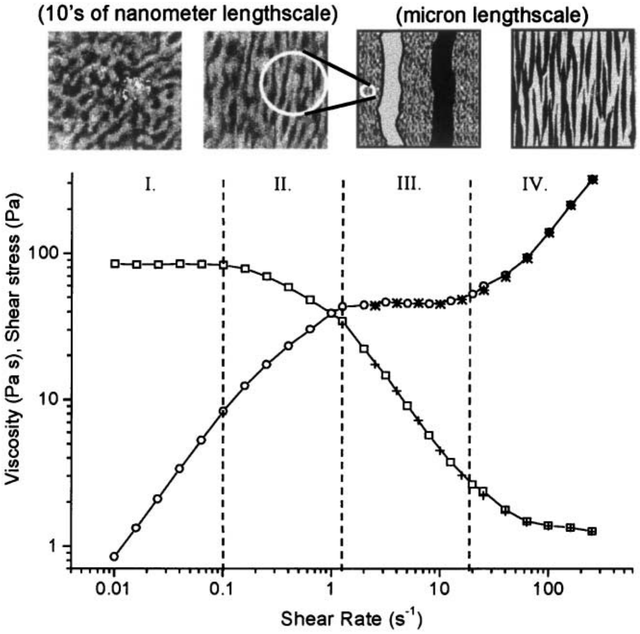

FIG. 1. Steady shear rheological data at 15 °C, showing the viscosity (□) and shear stress (○) as a function of shear rate. Data collected in the reverse direction, i.e., with decreasing rates, are shown as (+) and (∗), respectively. The insets represent the schematics of the hypothesized fluid structure in each of the four flow regimes.

instrument at NIST (Gaithersburg, MD), using a quartz Couette shear cell. The incident neutron beam ($\lambda = 12$ Å and $\Delta\lambda/\lambda = 0.11$) passes through this cell in the radial direction, with a total sample thickness of 1 mm. The SALS measurements were performed by using a Linkam shear stage, which employs a rotating parallel disk flow with transparent plates. A He-Ne laser beam ($\lambda = 632.8$ nm) was directed through the flow along the gradient direction, and 2D SALS patterns were projected onto a frosted glass screen and imaged with a CCD camera. Real-space microscopic imaging used the same shear cell, mounted on an optical microscope (Olympus) with a long working distance objective.

In the quiescent state, and at shear rates within Regime I, 2D SANS patterns are isotropic (Fig. 2a) and characterized by a peak that is well described by the Teubner-Strey structure factor for BμE [11–13]. As the shear rate increases into Regime II, the patterns become anisotropic, reflecting a suppression of scattered intensity along the flow direction (Fig. 2b). In Regime III, the anisotropic microemulsion pattern is accompanied by a streak of increased scattering intensity at low q oriented perpendicular to the flow direction (Figs. 2c and 2d), indicating the formation of anisotropic structures at larger length scales. This low q scattering increases in intensity throughout Regime III and into Regime IV (Figs. 2e and 2f). At high rates within Regime IV, there is complete loss of intensity at high q (i.e., in the range of the original microemulsion peak). Further increase of shear rate leads to saturation in the scattering intensity at low q.

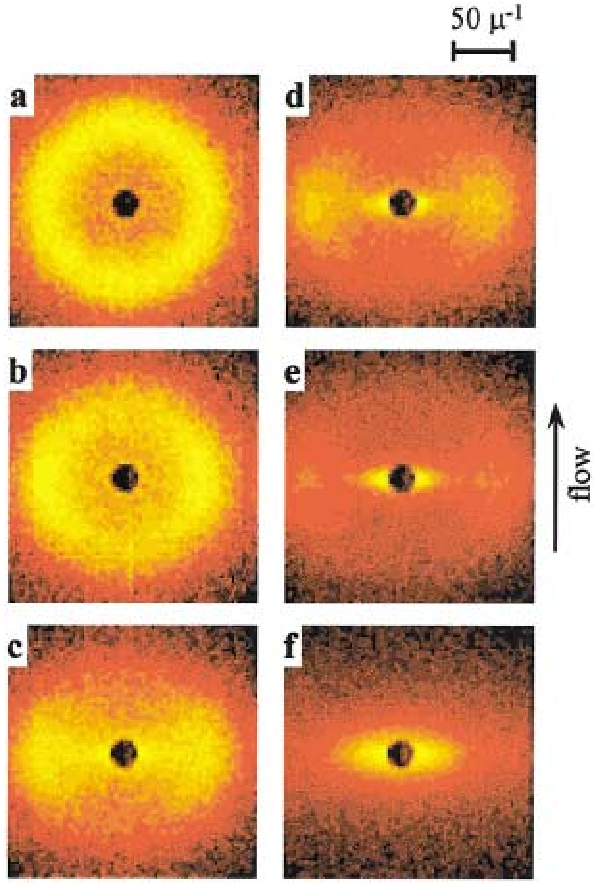

FIG. 2 (color). 2D SANS patterns at different shear rates ($T = 15$ °C) (a) 0, (b) 0.316, (c) 3.16, (d) 10, (e) 31.6, and (f) 316 s^{-1}. Data were collected for 300 s for each image. The patterns are shown in false color with constant logarithmic intensity scale.

At rest, and within Regimes I and II, the sample is nearly optically clear, with only a faint blue tint due to light scattering from the microemulsion structure ($d = 2\pi/q^* \cong 78$ nm). The SALS patterns collected at these low rates show only stray background scattering (Fig. 3). Upon entering Regime III, a bright streak emerges in the SALS patterns, oriented perpendicular to the flow direction, which increases in intensity with increasing shear rate. Direct microscopic observation in Regime III shows highly elongated micron-size structures (top panel, Fig. 4a). Following flow cessation within Regime III, the elongated structures gradually break up, confirming the existence of multiple phases during flow (Fig. 4a). The droplets thus formed gradually redissolve as the blend returns to its equilibrium BμE morphology.

In Regime IV, a dark streak emerges in the SALS pattern, dividing it into two lobes, which progressively separate and become more diffuse with further increases in shear rate (Fig. 3). At the same time, the total scattering intensity weakens, although this is likely due in part to the increasing overall turbidity. Optical microscopic observation at high rates also becomes difficult due to high turbidity, and only a dark featureless image is obtained (top panel, Fig. 4b). At higher illumination, fine striations may

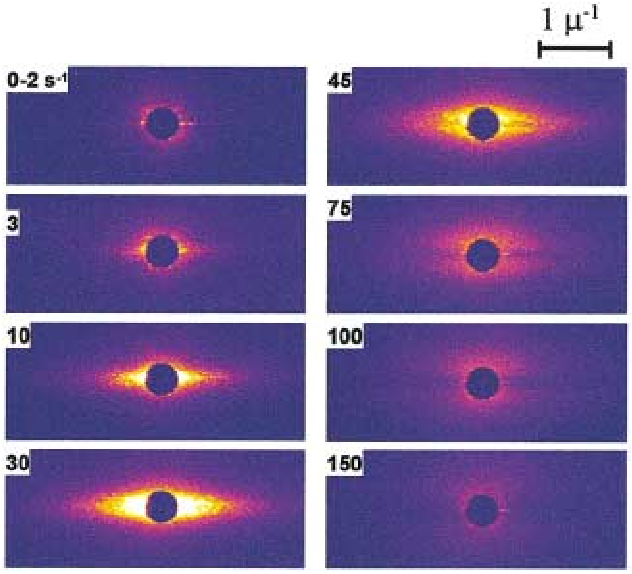

FIG. 3 (color). Steady SALS patterns at different shear rates ($T = 15\,^\circ$C, sample thickness equals 450 μm). The flow direction is vertical. The patterns are shown in false color with the same linear intensity scale.

still be observed within the overall dark images. Structural relaxation in Regime IV occurs by a very different mechanism than in Regime III. Upon flow cessation, there is a rapid overall increase in the image brightness, accompanied by fine-scale heterogeneity (Fig. 4b). As time progresses there is some coarsening in this fine structure, but also a progressive weakening in contrast as the sample returns to the BμE phase. The short time structural progression in Fig. 4b resembles the relaxation of immiscible polymer blends that have been sheared at high rates, in which spinodal-type structures are observed shortly after flow cessation [14]. However, unlike the binary blends where there is macroscopic phase separation at long times, these structures gradually remix to form the BμE.

The insets in Fig. 1 schematically illustrate hypotheses for the morphological transitions occurring through these regimes. Regime II is characterized by a distortion of the microemulsion. The interface with its normal parallel to the flow direction is exposed to the velocity gradient and is deformed and/or rotated away from this orientation, accounting for the loss of SANS intensity along the flow direction. This has the effect of reducing the degree of percolation of the bicontinuous structure in the velocity gradient direction, which should lead to a viscosity reduction, particularly since there is very high viscosity contrast between the two homopolymers (at 15 °C, $\eta_{\mathrm{PEE}} = 1500\eta_{\mathrm{PDMS}}$). At the same time, this distortion of interface places the BμE under increasing duress, since its equilibrium structure is optimized between a swollen lamellar structure and bulk phase separation.

We hypothesize that, beyond a critical shear stress, the BμE cannot withstand further deformation and submits to phase separation. The stress plateau in Fig. 1 corresponds to this critical stress level. Stress plateaus have attracted considerable interest, particularly in wormlike surfactant micelles. They have been interpreted either via a shear banding instability resulting from a nonmonotonic dependence of shear stress on shear rate in a single fluid phase [15] or in terms of a shear-induced transition between distinct fluid phases [2,16]. Direct microscopic visualization (Fig. 4a) provides conclusive evidence for the existence of multiple fluid phases within the stress plateau observed here. Within Regime III, we suspect that the critically deformed microemulsion remains the continuous phase, while increasing amounts of minority phase(s) are ejected in response to increases in shear rate as a stress limiting mechanism. This is consistent with the increasing SALS intensity with shear rate in this regime and the fact that SANS patterns continue to show the anisotropic

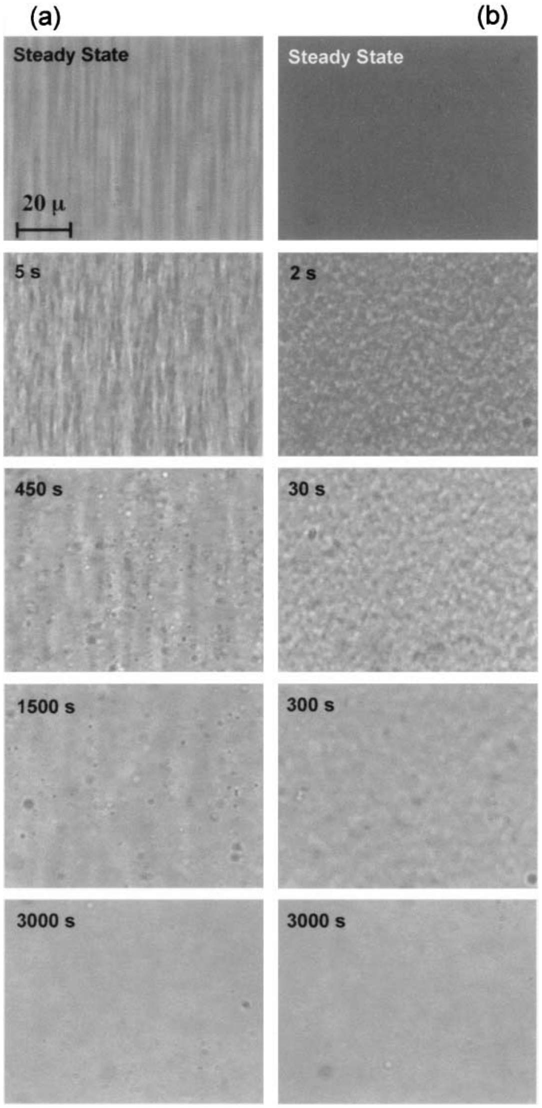

FIG. 4. Video microscopy images of structural relaxation upon cessation of shear flow within (a) Regime III (7.5 s^{-1}) and (b) Regime IV (150 s^{-1}). $T = 15\,^\circ$C; the sample thickness equals 800 μm for (a) and 450 μm for (b). The intensity scale is the same for all images within a set.

microemulsion scattering peak even as the low q scattering grows. This mechanism makes particular sense if one of the phases is PDMS-rich, since PDMS has a much lower viscosity than the BμE and hence will contribute negligibly to the overall viscosity. However, the overall symmetry of the phase diagram and close proximity to a three-phase region [17] suggest that Regime III may indeed be a shear-induced transition to a *three*-phase state, in which both PEE and PDMS homopolymers are ejected from the BμE, and in which (perhaps) excess block copolymer is solubilized in the homopolymers either as free molecules or micelles.

SANS shows the loss of all remnants of BμE scattering at sufficiently high shear rates in Regime IV. At the same time, there is still very strong low q scattering, and high sample turbidity. In this limit, we believe the ternary blend has been fully transformed into two nonequilibrium phases, rich in PEE and PDMS, with the block copolymer at the interface or solubilized within the homopolymers. The structure and rheology in this regime are then similar to that typically observed in immiscible blends. The details of the transition between Regimes III and IV are not clear. SANS suggests that the BμE is only fully destroyed at a rate between 31 and 100 s^{-1}, rates above the III/IV transition where stress is again increasing with shear rate. If the stress plateau is set by the maximum stress that can be sustained in the deformed BμE, it is possible that the end of the plateau corresponds to the point where the BμE stops being the continuous phase and hence ceases to control the stress level in the sample as a whole. In this case, the III/IV transition does not correspond directly to the final destruction of the BμE phase.

Polymeric BμEs occupy a narrow composition range intermediate between lamellar block copolymer structures, with organization at the nanometer-scale, and phase-separated polymer blends, which typically exhibit micron-scale multiphase morphology. Shear flow of this microemulsion leads to flow-induced structural phenomena that similarly bridge this gap between nanostructure and macrostructure. However, these complex phenomena are yet to be fully understood, and are distinct from the behavior of related classes of complex fluids. One report on block copolymer blended with the corresponding homopolymers [18] indicates that shear flow stabilizes the ordered phase. Studies on sponge phases [1] have shown a flow-induced transition to the lamellar phase. It is intriguing why the sponge phase goes lamellar, but the BμE phase separates; one factor could be the low solubility of the low molecular weight surfactant in water. Another reason may be that the sponge phase consists of only two components, whereas the BμE has three, the additional degree of freedom facilitating phase separation. Oil/water/surfactant BμEs [19] exhibit shear thinning at very high rates, attributed to pinching off of conduits along the shear gradient direction. The critical shear rate for the onset of shear thinning in the $o/w/s$ BμE was typically 2000 s^{-1}, whereas it was about 0.1 s^{-1} for our polymeric system. Thus the maximum relaxation times in the two systems can differ by as much as 4 orders of magnitude. This underscores [11] the convenience of having a polymeric system as a model for studying the dynamics and rheological behavior of BμE.

This work was supported by the MRSEC program of the NSF under DMR-9809364, at the University of Minnesota. We acknowledge David Giles for assistance with rheology, Bryan Chapman and Tanya Slawecki for help with SANS, and David Morse for helpful discussions.

[1] H. F. Mahjoub, C. Bourgaux, P. Sergot, and M. Kleman, Phys. Rev. Lett. **81**, 2076 (1998); J. Yamamoto and H. Tanaka, Phys. Rev. Lett. **77**, 4390 (1996).

[2] J.-F. Berret, D. C. Roux, and P. Lindner, Eur. Phys. J. B **5**, 67 (1998).

[3] C. R. Safinya, E. B. Sirota, R. F. Bruinsma, C. Jeppesen, R. J. Plano, and L. J. Wenzel, Science **261**, 588 (1993).

[4] K. Koppi, M. Tirrell, and F. S. Bates, Phys. Rev. Lett. **70**, 1449 (1993).

[5] V. K. Gupta, R. Krishnamoorti, J. A. Kornfield, and S. D. Smith, Macromolecules **28**, 4464 (1995).

[6] B. J. Ackerson and N. A. Clark, Phys. Rev. Lett. **46**, 123 (1981).

[7] E. Moses, T. Kume, and T. Hashimoto, Phys. Rev. Lett. **72**, 2037 (1994); X.-L. Wu, D. J. Pine, and P. K. Dixon, Phys. Rev. Lett. **66**, 2408 (1991).

[8] J.-W. Yu, J. F. Douglas, E. K. Hobbie, S. Kim, and C. C. Han, Phys. Rev. Lett. **78**, 2664 (1997); Z. Hong, M. T. Shaw, and R. A. Weiss, Macromolecules **31**, 6211 (1998); H. Gerard, J. S. Higgins, and N. Clarke, Macromolecules **32**, 5411 (1999).

[9] F. S. Bates, W. W. Maurer, P. M. Lipic, M. A. Hillmyer, K. Almdal, K. Mortensen, G. H. Fredrickson, and T. P. Lodge, Phys. Rev. Lett. **79**, 849 (1997).

[10] L. Kielhorn and M. Muthukumar, J. Chem. Phys. **107**, 5588 (1997).

[11] M. A. Hillmyer, W. W. Maurer, T. P. Lodge, F. S. Bates, and K. Almdal, J. Phys. Chem. B **103**, 4814 (1999).

[12] T. L. Morkved, B. R. Chapman, F. S. Bates, T. P. Lodge, P. Stepánek, and K. Almdal, Faraday Discuss. **112**, 335 (1999).

[13] M. Teubner and R. Strey, J. Chem. Phys. **87**, 3195 (1987).

[14] L. Kielhorn, R. H. Colby, and C. C. Han, Macromolecules **33**, 2486 (2000).

[15] N. A. Spenley, M. E. Cates, and T. C. B. McLeish, Phys. Rev. Lett. **71**, 939 (1993).

[16] P. D. Olmsted and C.-Y. D. Lu, Phys. Rev. E **56**, R55 (1997).

[17] N. R. Washburn, T. P. Lodge, and F. S. Bates, J. Phys. Chem. B **104**, 6987 (2000).

[18] A. I. Nakatani, L. Sung, E. K. Hobbie, and C. C. Han, Phys. Rev. Lett. **79**, 4693 (1997).

[19] M. R. Anklam, R. K. Prud'homme, and G. G. Warr, AIChE. J. **41**, 677 (1995).